RSC Advances

PAPER

View Article Online
View Journal | View Issue

Cite this: *RSC Adv.*, 2025, **15**, 7332

Microwave-assisted reductive homocoupling of aromatic nitro monomers: synthesis of azo-linked porous organic polymers for CO_2 capture†

Željka Car, Mladen Borovina, Barbara Panić and Ivana Biljan *

An optimized protocol for the rapid synthesis of azo-linked porous organic polymers (POPs) containing trigonal triphenylpyridine (AZO-P-M), triphenyltriazine (AZO-T-M), and tetragonal tetraphenylethylene (AZO-E-M) central units by microwave-assisted $NaBH_4$-mediated reductive homocoupling of the corresponding aromatic nitro monomers is presented. The structural and functional features of the azo-linked polymers prepared under microwave heating were directly compared to their counterparts obtained by conventional synthesis. Similar to azo-linked polymers synthesized by conventional reductive homocoupling of nitro monomers with $NaBH_4$, the polymers prepared under microwave irradiation are amorphous solids of good thermal stability showing moderate (*e.g.*, AZO-E-M with BET surface area of 302.1 $m^2\ g^{-1}$) to modest (*e.g.*, AZO-P-M with BET surface area of 22.9 $m^2\ g^{-1}$) porosities. Although the microwave-assisted procedure for the synthesis of azo-linked polymers described in this work did not result in systems with improved porosities, their efficiency for CO_2 adsorption (up to 29 mg g^{-1} at 306 K) is comparable to that of POPs synthesized by conventional heating. Therefore, the herein reported protocol could be used for the fast and efficient synthesis of new azo-linked POPs with potential for CO_2 capture.

Received 17th January 2025
Accepted 1st March 2025

DOI: 10.1039/d5ra00410a

rsc.li/rsc-advances

Introduction

Porous organic polymers (POPs) constitute a family of porous materials, constructed by linking organic building units *via* covalent bonds.[1–3] POPs can be categorized into several distinct groups, including crystalline covalent organic frameworks (COFs)[4–6] and covalent triazine frameworks (CTFs),[7,8] and amorphous hyper-cross-linked polymers (HCPs),[9] conjugated microporous polymers (CMPs),[10,11] porous polymer networks (PPNs),[12,13] polymers of intrinsic microporosity (PIMs)[14,15] and porous aromatic frameworks (PAFs).[16,17] The remarkable features of POPs, such as their high and permanent porosity, high chemical and thermal stability, low density, and tuneable structure and functionality, offer possibilities for various applications, *e.g.*, in gas storage and separation, energy storage and conversion, catalysis, sensing and drug delivery.[18–28] Noteworthily, POPs are considered as prime candidates for the selective adsorption and capture of carbon dioxide (CO_2),[2,18–20,29] whose elevated emissions into the atmosphere have become a major environmental challenge due to their contribution to climate change.[30,31] The ability of POPs to adsorb CO_2 can be tailored by introducing specific functionalities into the porous framework.[32,33] Since CO_2 has a much higher quadrupole moment compared to most other gases, including nitrogen (N_2), incorporation of polar functional groups and Lewis basic sites (*e.g.*, nitrogen-rich moieties) into POPs can provide favourable interactions with CO_2 leading to enhanced CO_2 uptake capacity and selectivity.[34–42] Among the promising materials for post-combustion CO_2 capture are azo-linked POPs which show high CO_2/N_2 selectivity with increase in temperature as reported by Patel *et al.*[37,38] Namely, it was suggested that besides acting CO_2-philic, azo groups show less than expected affinity towards N_2 gas, thus making the framework N_2-phobic.[38] Such combination of CO_2-philicity and N_2-phobicity can be used for efficient CO_2 capture and separation. Azo-linked POPs are usually synthesized by heterocoupling of aromatic nitro and amino monomers under basic conditions,[37,38] by copper(I)-catalyzed oxidative homocoupling of aromatic amino monomers,[43,44] and by Zn- or $NaBH_4$-mediated reductive homocoupling of aromatic nitro monomers.[45,46] Heterocoupling method as well as copper(I)-catalyzed oxidative homocoupling and Zn-induced reductive homocoupling require long reaction time of 24 h, 48 h and 36 h, respectively.[37,38,43–45] $NaBH_4$-mediated reductive homocoupling of four-folded tetragonal and tetrahedral monomers containing nitro groups has been shown to be much more time-efficient with a reported reaction time of 30 min and high yields.[46] However, the same synthetic approach was significantly time-consuming for the synthesis of azo-linked POP with trigonal triphenyltriazine central unit with

Department of Chemistry, Faculty of Science, University of Zagreb, Horvatovac 102a, HR-10000 Zagreb, Croatia. E-mail: ibiljan@chem.pmf.hr

† Electronic supplementary information (ESI) available. See DOI: https://doi.org/10.1039/d5ra00410a

the reaction time of 24 h.[47] These previously reported $NaBH_4$-mediated reductive homocoupling reactions of various aromatic polynitro monomers have been carried out by conventional heating. Moreover, to the best of our knowledge, there are no literature reports on the synthesis of azo-linked POPs using environmentally friendly approaches such as microwave heating. In general, POPs are mainly synthesized by conventional methods.[48] Microwave-assisted synthesis has proven to be fast and efficient method for obtaining compounds in agreement with green chemistry principles. The reactions performed under microwave conditions are characterized by high yields and short reaction times because of rapid heating and energy transfer directly into reaction medium.[49] Nowadays, microwave-assisted synthesis is used for various multicomponent reactions, in solid state chemistry, nanomaterial synthesis, organic synthesis, polymer synthesis and drug discovery.[8,48,50–52]

Herein, we report for the first time a facile and rapid microwave-assisted synthesis of azo-linked polymers with trigonal triphenylpyridine (AZO-P-M), triphenyltriazine (AZO-T-M), and tetragonal tetraphenylethylene (AZO-E-M) central units *via* $NaBH_4$-mediated reductive homocoupling of the corresponding nitro monomers **1–3** (Fig. 1). The obtained polymers were thoroughly characterized by IR spectroscopy, ^{13}C CP/MAS NMR spectroscopy, powder X-ray diffraction (PXRD), elemental analysis, thermogravimetric analysis (TGA) and nitrogen (N_2) adsorption–desorption experiments. Structural and functional characteristics of polymers prepared under microwave-assisted conditions were compared to that of azo-linked polymers synthesized by $NaBH_4$-mediated reductive homocoupling with conventional heating. While the conventional synthesis of azo-linked polymers with triphenyltriazine (AZO-T-P2)[47] and tetraphenylethylene (Azo-POP-3)[46] central unit has been previously described in the literature, to allow a direct comparison, the synthesis of triphenylpyridine-based azo-linked polymer (AZO-P) using a conventional approach was carried out in this study.

Results and discussion

Synthesis of azo-linked polymers

As mentioned, conventional $NaBH_4$-mediated reductive homocoupling of four-folded tetragonal and tetrahedral nitro monomers has shown to be time-efficient with a reported reaction time of 30 min and high yields.[46] The reactions were typically performed by 15 min addition of $NaBH_4$ to nitro monomers in DMF and subsequent heating of the reaction mixture at 85 °C for additional 15 min. In our optimization process we used the above-mentioned conditions first in the microwave-assisted synthesis of AZO-P-M from **1** (entry 1, Table S1†). Only the starting material was isolated from the reaction mixture at these conditions. At 120 °C and 30 min 92% of product was obtained and approximately the same yield was achieved in 15 min of reaction time. Interestingly, when the reaction time was further shortened to 5 min the yield was reduced to 64%. But at 140 °C the reaction was completed within 5 min with 94% yield. Optimized conditions for AZO-P-M were used for the microwave-assisted synthesis of the other two azo-linked POPs, AZO-T-M and AZO-E-M from **2** and **3**, respectively. The final conditions (Table 1) for the synthesis of AZO-E-

Table 1 Final microwave conditions and yields for the synthesis of AZO-P-M, AZO-T-M and AZO-E-M (p = 300 psi, power 300 W)

Product	Time/min	T/°C	m/mg	Yield/%
AZO-P-M	5	140	110.3	94
AZO-T-M	15	120	111.6	95
AZO-E-M	5	140	109	97

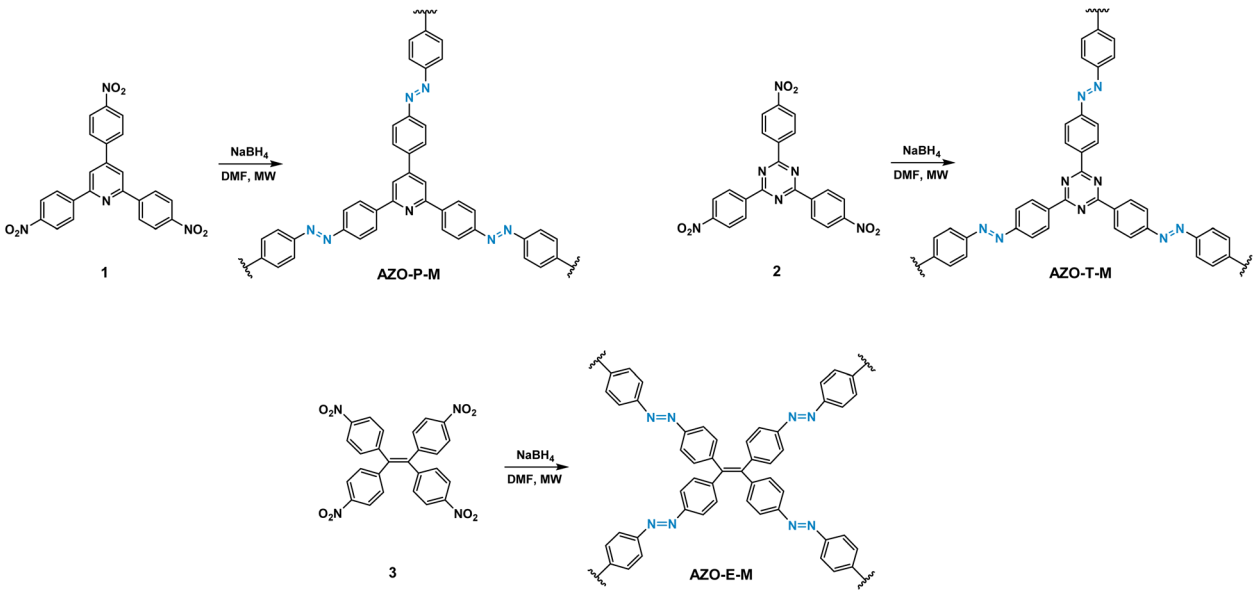

Fig. 1 Synthesis of azo-linked polymers AZO-P-M, AZO-T-M and AZO-E-M by $NaBH_4$-mediated reductive homocoupling of corresponding nitro monomers **1**, **2** and **3** under microwave conditions.

M were the same as those for the AZO-P-M. Thus, azo-linked polymer with tetraphenylethylene central unit was prepared within 5 min at 140 °C and with a high yield of 97%. In the preparation of AZO-T-M, the reduced reaction time to 5 min at 140 °C afforded only 68% of the product. The optimal conditions for the preparation of this compound were 15 min at 120 °C, which afforded AZO-T-M with a high yield of 95%.

When compared with the conventional synthesis, improvements in reaction times and yields under microwave conditions were observed for all three investigated azo-linked POPs. This is especially pronounced for the systems with trigonal triphenylpyridine and triphenyltriazine central units. In contrast to the previously reported time-efficient conventional synthesis of azo-linked POP based on tetragonal tetraphenylethylene units (Azo-POP-3),[46] which was completed after 30 min with 92% yield, the synthesis of AZO-P (see ESI, Fig. S1†) and AZO-T-P2 (ref. 47) using conventional approach required a significantly longer reaction time. Namely, after 30 min no polymeric products AZO-P and AZO-T-P2 could be detected in the reaction mixtures and the reactions were completed only after 24 hours. However, under microwave conditions the reaction times were shortened to 5 min for AZO-P-M and 15 min for AZO-T-M. This was also accompanied by increase in reaction yields from 79% for AZO-P to 94% for AZO-P-M, and from 37% for AZO-T-P2 to 95% for AZO-T-M. The reaction time for the microwave-assisted synthesis of AZO-E-M was only 5 min with a high yield of 97%, making this approach also more efficient for this compound compared to conventional synthesis, which was completed after 30 min with a yield of 92%.[46] The synthesized polymers are insoluble in common organic solvents (*e.g.*, acetone, DMF, THF, dichloromethane, methanol and DMSO), indicating formation of cross-linked frameworks.

Characterization of structural and functional properties of azo-linked polymers

Chemical and structural characterization of azo-linked pyridine, triazine and ethylene-based polymers was carried out by IR spectroscopy, ^{13}C CP/MAS NMR spectroscopy, powder X-ray diffraction (PXRD) and elemental analysis. Fig. 2 shows a comparison of FTIR spectra of AZO-P-M, AZO-T-M and AZO-E-M prepared under microwave conditions and starting nitro monomers. The appearance of bands at 1455 and 1423 cm^{-1}, 1438 and 1407 cm^{-1}, and 1446 and 1402 cm^{-1} in AZO-P-M, AZO-T-M and AZO-E-M, respectively, suggested formation of azo bonds. The FTIR spectrum of AZO-P prepared by conventional synthesis also revealed bands at 1454 and 1422 cm^{-1}, attributed to stretching vibrations of azo bonds (Fig. S2†). The position of azo bond stretching bands in the spectra of AZO-T-M and AZO-E-M matches with frequencies of the same vibration bands in the spectra of triazine and ethylene-based polymers prepared by conventional synthesis.[46,47] In addition, in the FTIR spectra of all synthesized polymers asymmetric and symmetric stretching vibrations bands of unreacted nitro groups were observed around 1500 and 1350 cm^{-1}.

The formation of azo-linked polymers was unequivocally confirmed by comparison of solid-state ^{13}C CP/MAS NMR spectra of polymeric products and starting nitro monomers (Fig. 3). Namely, the ^{13}C CP/MAS NMR spectra of AZO-P-M, AZO-T-M and AZO-E-M showed the new signal at 153.3, 153.9 and 151.5 ppm, respectively, attributed to the carbon directly bonded to the azo group (–C–N=N–). For comparison, chemical shifts of carbon atoms attached to the azo group in AZO-P (Fig. S3d†), AZO-T-P2 (ref. 47) and Azo-POP-3 (ref. 46) are situated at 153.1, 154.3 and 151.1 ppm, respectively. Furthermore, the ^{13}C CP/MAS spectra of the obtained polymers displayed the other characteristic signals of constituting units such as phenyl, pyridine, triazine and ethylene carbon signals. The broad diffraction peaks in the PXRD patterns of AZO-P-M, AZO-T-M and AZO-E-M indicated their amorphous nature (Fig. S4†), which is consistent with the PXRD data obtained for their counterparts synthesized by the conventional approach and other similar azo-linked POPs.[37,38,43,44,46,47,53–59]

Similarly to azo-linked POPs prepared by conventional heating, there are some differences between the experimentally determined and expected composition of AZO-P-M, AZO-T-M and AZO-E-M produced by the microwave-assisted synthesis. Such deviations are often observed with POPs and are probably due to incomplete polymerization and adsorption of moistures.[43,44,60]

The thermal stability of azo-linked polymers prepared under microwave conditions was determined using TGA by heating the samples in N_2 atmosphere up to 800 °C. To remove traces of residual solvents all samples were heated to 180 °C in N_2 atmosphere and held at isothermal conditions at 180 °C for 10 minutes. Compounds prepared *via* microwave-assisted synthesis show slightly lesser thermal stability and start to

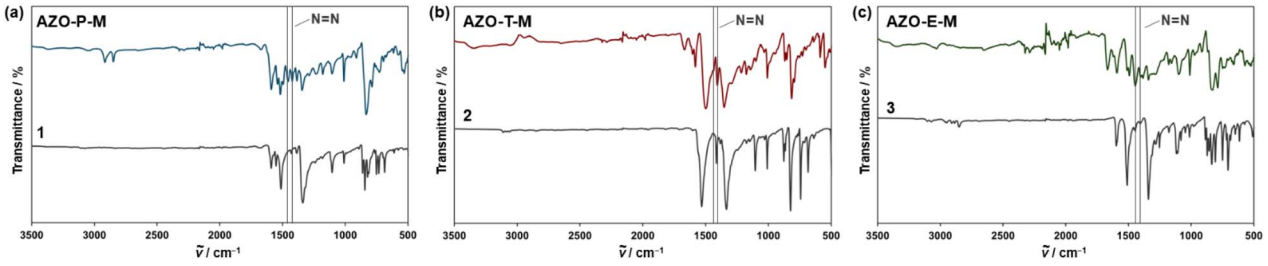

Fig. 2 Comparison of FTIR spectra of: (a) AZO-P-M and starting nitro compound **1**, (b) AZO-T-M and starting nitro compound **2** and (c) AZO-E-M and starting nitro compound **3**. Signals attributed to the stretching vibrations of the azo (–N=N–) group in polymers are marked with vertical lines.

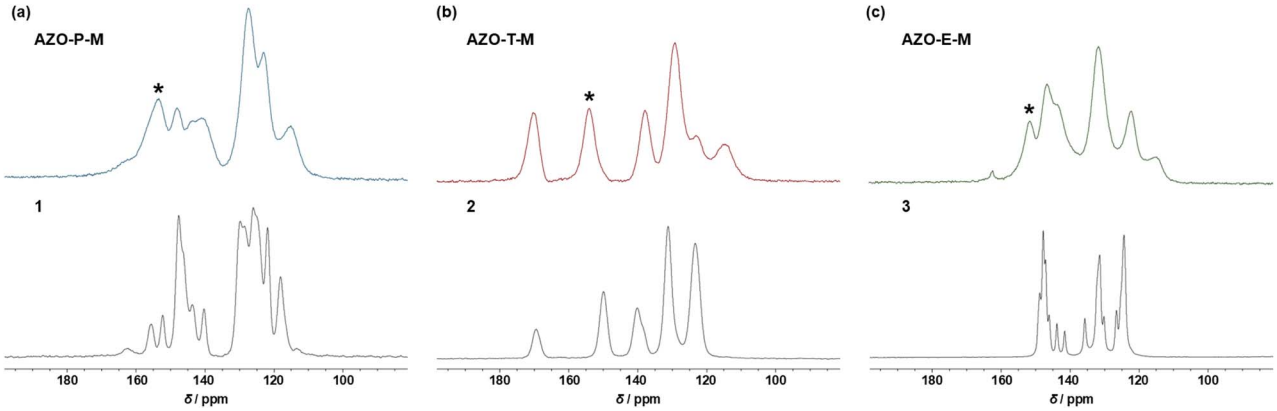

Fig. 3 Comparison of ^{13}C CP/MAS NMR spectra of: (a) AZO-P-M and starting nitro compound **1**, (b) AZO-T-M and starting nitro compound **2** and (c) AZO-E-M and starting nitro compound **3**. Signal of carbon atom directly attached to the azo group (–C–N=N–) in polymers is marked with asterisk (*).

decompose at temperatures 20 °C (AZO-E-M) to 50 °C (AZO-T-M) lower than their counterparts prepared by conventional synthesis (Fig. S5–S7†). They also exhibit some slight differences in decomposition events and rates. AZO-P-M shows a decrease in mass starting at around 200 °C and loses ~11.5% of its mass by 500 °C followed by an additional reduction of ~23% until 800 °C (Fig. S5†). Its counterpart AZO-P is stable until around 230 °C and loses ~5.8% of its mass by 500 °C followed by an additional reduction of ~19% until 800 °C (Fig. S5†). AZO-T-M shows a decrease in mass starting around 190 °C and loses ~7.7% of its mass by 470 °C followed by an additional reduction of ~24% (Fig. S6†). Its counterpart AZO-T-P2 is stable until around 250 °C and loses ~7.3% of mass by 490 °C followed by an additional ~42% reduction until 800 °C.[47] Both compounds lose less than 0.1 mg during the isothermal step at 800 °C. AZO-E-M starts exhibiting a decrease in mass at around 190 °C and loses ~10.4% by 480 °C, followed by an additional reduction of ~19% until 800 °C (Fig. S7†). Its counterpart Azo-POP-3 is stable until around 210 °C and loses ~15% of its mass by 470 °C followed by an additional reduction of ~30% until 800 °C.[46] The porosity features of AZO-P-M, AZO-T-M and AZO-E-M were investigated by N_2 adsorption–desorption measurements at 77 K (Fig. 4 and S8†) and compared to that of pyridine, triazine and ethylene-based polymers synthesized with conventional heating. The surface areas of AZO-P-M, AZO-T-M and AZO-E-M calculated based on the BET model exhibit wide range of values (Table 2). The highest BET surface area of 302.1 $m^2\ g^{-1}$ was obtained for AZO-E-M, built from tetragonal tetraphenylethylene units. However, this value is somewhat lower than BET surface area of Azo-POP-3 (497 $m^2\ g^{-1}$) prepared by conventional synthesis.[46] The BET surface areas of azo-linked polymers with trigonal triphenylpyridine (AZO-P-M) and triphenyltriazine (AZO-T-M) central units are significantly lower, being 22.9 and 1.1 $m^2\ g^{-1}$, respectively. While the BET surface area of pyridine-based AZO-P-M synthesized by microwave heating is higher than that of the AZO-P (2.1 $m^2\ g^{-1}$) prepared by conventional heating, the reverse trend was observed for the triazine-based azo-linked polymers AZO-T-M and AZO-T-P2. Surprisingly, the BET surface area of AZO-T-M (1.1 $m^2\ g^{-1}$) is much lower than that of AZO-T-P2 (351 $m^2\ g^{-1}$),[47] prepared by conventional synthesis. According to the pore size distribution, AZO-E-M mostly contains micropores and mesopores (Fig. 4b), while AZO-P-M and AZO-T-M possess mesopores and macropores (Fig. S8†). The recorded N_2 adsorption–desorption isotherms supported this observation. All three polymers, AZO-P-M, AZO-T-M and AZO-E-M, show type IV isotherms according to the IUPAC classification, which is typical for mesoporous materials. The occurrence of hysteresis is common for type IV isotherms. Polymers AZO-P-M and AZO-T-M possess H3 hysteresis loops usually associated with materials that have

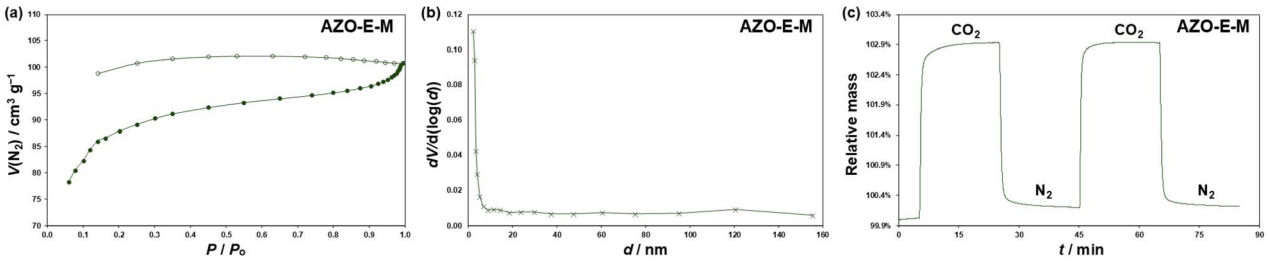

Fig. 4 (a) Representative N_2 adsorption–desorption isotherms of AZO-E-M measured at 77 K. The adsorption and desorption isotherms are depicted with filled and open markers, respectively. (b) Representative pore size distribution of AZO-E-M. (c) Representative thermogravimetric CO_2 adsorption and desorption profiles of AZO-E-M at approximately 306 K.

Table 2 Comparison of BET surface areas and CO_2 uptakes of azo-linked polymers synthesized by different methods

Compound	S_{BET} ($m^2\ g^{-1}$)	CO_2 uptake (mg g^{-1})	Synthetic method
AZO-P-M	22.9	21	MW $NaBH_4$-mediated reductive homocoupling
AZO-T-M	1.1	20	MW $NaBH_4$-mediated reductive homocoupling
AZO-E-M	302.1	29	MW $NaBH_4$-mediated reductive homocoupling
AZO-P	2.1	24	$NaBH_4$-mediated reductive homocoupling
AZO-T-P2[a]	350.9	22	$NaBH_4$-mediated reductive homocoupling
Azo-POP-3[b]	497	Not measured	$NaBH_4$-mediated reductive homocoupling
TPP-azo[c]	606	32	Cu(I)-catalyzed oxidative homocoupling
ALP-4[d]	862	81	Cu(I)-catalyzed oxidative homocoupling
ALP-8[e]	517	87	Cu(I)-catalyzed oxidative homocoupling
Azo-POF-2[f]	439	55	Zn-mediated reductive homocoupling
Azo-COP-1[g]	635	27	Heterocoupling
Azo-COP-2[g]	729	31	Heterocoupling
Azo-COP-3[g]	493	15	Heterocoupling

[a] Ref. 47. [b] Ref. 46. [c] Ref. 53. [d] Ref. 43. [e] Ref. 44. [f] Ref. 45. [g] Ref. 37.

macropores that are not completely filled with condensed gas (Fig. S8†). The H4 hysteresis loop present in AZO-E-M is typical for materials with filled micropores (Fig. 4a).

Next, we investigated the CO_2 adsorption performance of the synthesized azo-linked polymers by TGA at approximately 306 K. The obtained CO_2 adsorption capacities are listed in Table 2. Compounds AZO-P-M, AZO-E-M, AZO-P and AZO-T-P2 show similar CO_2 adsorption behaviour with relatively sharp increases in mass in CO_2 atmosphere and sharp decreases in mass in N_2 atmosphere (Fig. 4c, S9a, c and d†). Compound AZO-T-M (Fig. S9b†) shows a distinct adsorption behaviour from its counterpart AZO-T-P2 (Fig. S9d†). As is the case with other measured compounds, AZO-T-M shows a gradual increase in mass during the first CO_2 cycle then a decrease in mass during the N_2 cycle that stops before it reaches baseline values, and it retains an increased mass corresponding to 0.5% of the initial sample mass. CO_2 uptake during the second cycle is more pronounced and the sample becomes saturated much sooner. The decrease of the mass during the second N_2 cycle shows similar behaviour as it did in the first cycle. Baseline values were not reached, and the sample retained an increase of 0.5% of its starting mass.

The highest CO_2 uptake value of 29 mg g^{-1} was obtained for AZO-E-M, which has also the highest BET surface area among the studied systems. Although AZO-P-M and AZO-T-M have significantly lower BET surface areas compared to AZO-E-M, the difference in CO_2 uptake capacities of these three systems is less noticeable. Namely, AZO-P-M and AZO-T-M display CO_2 uptake capacities of 21 and 20 mg g^{-1}, respectively. These results are in accordance with the previous findings which indicated that the high BET surface area value is not a decisive factor for the affinity towards CO_2 adsorption.[38,40,61] The presence of CO_2-philic nitrogen rich functionalities in AZO-P-M and AZO-T-M appears to contribute most to their affinity for CO_2. This is strongly corroborated by comparing the CO_2 uptake values of AZO-P-M and AZO-T-M and their counterparts, AZO-P and AZO-T-P2, prepared by conventional synthesis. Although the polymer pairs synthesised under microwave and conventional heating show significantly different BET surface area values, their CO_2 adsorption capacities are very similar (21 mg g^{-1} for AZO-P-M and 24 mg g^{-1} for AZO-P, and 20 mg g^{-1} for AZO-T-M and 22 mg g^{-1} for AZO-T-P2).[47] The CO_2 uptake capacities of azo-linked polymers prepared by microwave-assisted $NaBH_4$-mediated reductive homocoupling of aromatic nitro monomers are comparable (AZO-E-M) or somewhat lower (AZO-P-M and AZO-T-M) to that of pyridine-based TPP-azo (32 mg g^{-1} at 303 K),[53] and much lower than that of benzene-based azo-linked ALP-4 (81 mg g^{-1} at 298 K)[43] and ethylene-based ALP-8 (1.97 mmol g^{-1}, 87 mg g^{-1}, at 298 K),[44] which were prepared by Cu(I)-catalysed oxidative homocoupling of corresponding amino monomers (Table 2). In addition, they are somewhat lower compared to ethylene-based azo-linked Azo-POF-2 (55.1 mg g^{-1} at 298 K),[45] prepared by Zn-induced reductive homocoupling of nitro monomer, but comparable to azo-COPs (15–31 mg g^{-1} at 323 K),[37] incorporating 3D tetrahedral building units which were prepared by heterocoupling of aromatic nitro and amino monomers (Table 2).

Experimental

General information

All chemicals were used as received from the suppliers. Compounds **1**, **2** and **3** were prepared as previously described.[46,62,63] The solvents were purified or dried according to the literature procedures. Microwave-assisted synthesis was performed on a Discover SP microwave reactor equipped with an autosampler, IR temperature sensor, and integrated camera (CEM Corporation). The synthesized compounds were identified by solution ^1H NMR spectroscopy, solid-state ^{13}C CP/MAS NMR spectroscopy, IR spectroscopy, PXRD and elemental analysis. Solution-state ^1H NMR spectra were recorded on a Bruker Ascend 400 MHz NMR spectrometer at 25.0 °C. DMSO-d_6 was used as a solvent and TMS as an internal standard for chemical shifts. Solid-state ^{13}C CP/MAS NMR spectra were recorded on a Bruker Avance III HD 400 MHz NMR spectrometer at spinning rate of 15 kHz. FTIR spectra were recorded on a PerkinElmer UATR Two spectrometer in the spectral range between 4000 cm^{-1} and

400 cm^{-1} at a resolution of 4 cm^{-1}, averaging 10 scans per spectrum. Elemental analysis was provided by the Analytical Services Laboratory of the Ruđer Bošković Institute, Zagreb, Croatia. PXRD diffractograms were recorded on a Malvern Panalytical Aeris powder diffractometer in Bragg–Brentano geometry with PIXcel1D detector. Thermogravimetric analysis was carried out using a simultaneous TGA-DTA analyser Mettler-Toledo TGA/DSC 3+. Samples were placed in alumina pans (70 μL) and heated in flowing nitrogen (50 mL min^{-1}) from 30 °C up to 180 °C at a rate of 10 °C min^{-1} and held in isothermal conditions for 10 minutes at 180 °C to remove traces of solvents. Afterwards, samples were cooled to room temperature and heated in flowing nitrogen (50 mL min^{-1}) from 25 °C up to 800 °C at a rate of 10 °C min^{-1} and held in isothermal conditions for 15 minutes at 800 °C. CO_2 sorption experiments were carried out by following a previously reported procedure with minor modifications in experimental conditions.[64] Before performing CO_2 adsorption experiments, a 70 μL alumina pan was filled with a fresh sample, heated to 100 °C at a heating rate of 20 °C min^{-1} in nitrogen atmosphere (flow rate 150 mL min^{-1}) and held at 100 °C for 30 minutes to dry the sample. After drying, CO_2 adsorption was measured by switching between N_2 atmosphere and CO_2 atmosphere in 20 min intervals (flow rates for both gases were 150 mL min^{-1}) at ~30 °C. The measured sample temperature varied around 33 °C during CO_2 cycles. To correct for different buoyancy effects on the TG scale and alumina pan, a baseline curve was recorded under the same experimental conditions using an empty alumina pan and subtracted from the measured curve. Data collection and analysis were performed using the program package STAR^e Software 16.40 Mettler Toledo GmbH. The specific surface area was determined from N_2 gas adsorption–desorption data obtained with Micromeritics ASAP-2000 at 77 K at a relative pressure (p/p_0) range of 0.06–0.99.[65,66] Before analysis, samples were degassed at 150 °C under a dynamic vacuum of 7 mPa. The adsorption data were used to calculate the surface area from the linear range of the BET equation, while the pore size distribution was determined using the Barrett–Joyner–Halenda (BJH) method.

Synthesis

In a typical microwave procedure, to a 150 mg of each nitro compound (**1**, **2** or **3**) in 35 mL Pyrex pressure vessel, $NaBH_4$ (3 equiv. for **1** and **2**; 4 equiv. for **3**) as well as DMF (10 mL) were added. Detailed final conditions and yields for each reaction are listed in Table 1. After reaction completion water was added (10 mL) to the vessel and the resulting swelling precipitate of brown-red colour was filtered off. It was washed excessively with water and acetone first and then with DMF and THF. The amorphous product of each reaction was dried and characterized by IR and solid-state ^{13}C CP/MAS NMR spectroscopy, and elemental analysis.

Conclusions

We report for the first time, to the best of our knowledge, a rapid microwave-assisted synthesis of pyridine, triazine and ethylene-based azo-linked POPs *via* $NaBH_4$-mediated reductive homocoupling of the corresponding aromatic nitro monomers. The obtained polymers showed similar structural and thermal characteristics as their counterparts synthesized by conventional heating and other similar azo-linked POPs. They are mostly mesoporous materials with the BET surface areas exhibiting various values. While the azo-linked polymer bearing tetragonal tetraphenylethylene central unit showed moderate BET surface area of 302.1 m^2 g^{-1}, systems with trigonal triphenylpyridine and triphenyltriazine central units displayed significantly lower values of 22.9 and 1.1 m^2 g^{-1}, respectively. Nevertheless, their CO_2 adsorption capacities are roughly comparable being distributed from 20 to 29 mg g^{-1} at 306 K. These results further support previous findings that the favourable interactions between the nitrogen-rich CO_2-philic functionalities and CO_2 have a significant contribution to the affinity of POPs for this main greenhouse gas. The herein optimized microwave-assisted protocol could be used for the efficient and fast synthesis of various functional azo-linked polymers.

Data availability

The data supporting this article have been included as part of the ESI.†

Author contributions

Conceptualisation, I. B.; methodology, Ž. C., M. B. and I. B.; validation, Ž. C. and I. B.; investigation, Ž. C., M. B., B. P. and I. B.; writing – original draft preparation, Ž. C., M. B., B. P. and I. B.; writing – review and editing, I. B.; visualisation, Ž. C., M. B., B. P. and I. B.; supervision, I. B.; project administration, I. B.; funding acquisition, I. B. All authors have given approval to the final version of the manuscript.

Conflicts of interest

There are no conflicts to declare.

Acknowledgements

This work has been fully supported by Croatian Science Foundation under the project IP-2020-02-4467. The support of project CIuK (Grant KK.01.1.1.02.0016) co-financed by the Croatian Government and the European Union through the European Regional Development Fund – Competitiveness and Cohesion Operational Program is acknowledged.

Notes and references

1 S. Das, P. Heasman, T. Ben and S. Qiu, *Chem. Rev.*, 2017, **117**, 1515–1563.
2 M. G. Mohamed, A. F. M. EL-Mahdy, M. G. Kotp and S.-W. Kuo, *Mater. Adv.*, 2022, **3**, 707–733.
3 Z. Zhang, Z. Liu, C. Xue, H. Chen, X. Han and Y. Ren, *Commun. Chem.*, 2023, **6**, 271.

4 K. Geng, T. He, R. Liu, S. Dalapati, K. T. Tan, Z. Li, S. Tao, Y. Gong, Q. Jiang and D. Jiang, *Chem. Rev.*, 2020, **120**, 8814–8933.
5 N. Huang, P. Wang and D. Jiang, *Nat. Rev. Mater.*, 2016, **1**, 16068.
6 R. Liu, K. T. Tan, Y. Gong, Y. Chen, Z. Li, S. Xie, T. He, Z. Lu, H. Yang and D. Jiang, *Chem. Soc. Rev.*, 2021, **50**, 120–242.
7 P. Kuhn, M. Antonietti and A. Thomas, *Angew. Chem., Int. Ed.*, 2008, **47**, 3450–3453.
8 S. Ren, M. J. Bojdys, R. Dawson, A. Laybourn, Y. Z. Khimyak, D. J. Adams and A. I. Cooper, *Adv. Mater.*, 2012, **24**, 2357–2361.
9 L. Tan and B. Tan, *Chem. Soc. Rev.*, 2017, **46**, 3322–3356.
10 N. Chaoui, M. Trunk, R. Dawson, J. Schmidt and A. Thomas, *Chem. Soc. Rev.*, 2017, **46**, 3302–3321.
11 J.-S. M. Lee and A. I. Cooper, *Chem. Rev.*, 2020, **120**, 2171–2214.
12 W. Lu, D. Yuan, D. Zhao, C. I. Schilling, O. Plietzsch, T. Muller, S. Bräse, J. Guenther, J. Blümel, R. Krishna, Z. Li and H.-C. Zhou, *Chem. Mater.*, 2010, **22**, 5964–5972.
13 D. Yuan, W. Lu, D. Zhao and H. Zhou, *Adv. Mater.*, 2011, **23**, 3723–3725.
14 N. B. McKeown and P. M. Budd, *Chem. Soc. Rev.*, 2006, **35**, 675.
15 N. B. McKeown and P. M. Budd, *Macromolecules*, 2010, **43**, 5163–5176.
16 Y. Tian and G. Zhu, *Chem. Rev.*, 2020, **120**, 8934–8986.
17 T. Ben and S. Qiu, *CrystEngComm*, 2013, **15**, 17–26.
18 P. Bhanja, A. Modak and A. Bhaumik, *ChemCatChem*, 2019, **11**, 244–257.
19 K. S. Song, P. W. Fritz and A. Coskun, *Chem. Soc. Rev.*, 2022, **51**, 9831–9852.
20 G. Singh, J. Lee, A. Karakoti, R. Bahadur, J. Yi, D. Zhao, K. AlBahily and A. Vinu, *Chem. Soc. Rev.*, 2020, **49**, 4360–4404.
21 T. Zhang, G. Xing, W. Chen and L. Chen, *Mater. Chem. Front.*, 2020, **4**, 332–353.
22 D.-H. Yang, Y. Tao, X. Ding and B.-H. Han, *Chem. Soc. Rev.*, 2022, **51**, 761–791.
23 X. Liu, C. Liu, W. Lai and W. Huang, *Adv. Mater. Technol.*, 2020, 2000154.
24 S. Zhang, Q. Yang, C. Wang, X. Luo, J. Kim, Z. Wang and Y. Yamauchi, *Adv. Sci.*, 2018, **5**, 1801116.
25 Y. Tang, A. Varyambath, Y. Ding, B. Chen, X. Huang, Y. Zhang, D. Yu, I. Kim and W. Song, *Biomater. Sci.*, 2022, **10**, 5369–5390.
26 Y. Zhu, P. Xu, X. Zhang and D. Wu, *Chem. Soc. Rev.*, 2022, **51**, 1377–1414.
27 P. Kaur, J. T. Hupp and S. T. Nguyen, *ACS Catal.*, 2011, **1**, 819–835.
28 H. Wang, J. Sun, X. Cai and Y. Zhu, *Eur. J. Inorg. Chem.*, 2024, **27**, e202400254.
29 M. Sai Bhargava Reddy, D. Ponnamma, K. K. Sadasivuni, B. Kumar and A. M. Abdullah, *RSC Adv.*, 2021, **11**, 12658–12681.
30 K. O. Yoro and M. O. Daramola, in *Advances in Carbon Capture*, Elsevier, 2020, pp. 3–28.
31 L. J. R. Nunes, *Environments*, 2023, **10**, 66.
32 B. Gui, X. Liu, Y. Cheng, Y. Zhang, P. Chen, M. He, J. Sun and C. Wang, *Angew. Chem., Int. Ed.*, 2022, **61**, e202113852.
33 M. Perovic, Q. Qin and M. Oschatz, *Adv. Funct. Mater.*, 2020, **30**, 1908371.
34 Y. Zhu, H. Long and W. Zhang, *Chem. Mater.*, 2013, **25**, 1630–1635.
35 M. G. Rabbani and H. M. El-Kaderi, *Chem. Mater.*, 2012, **24**, 1511–1517.
36 C. Gu, D. Liu, W. Huang, J. Liu and R. Yang, *Polym. Chem.*, 2015, **6**, 7410–7417.
37 H. A. Patel, S. Hyun Je, J. Park, D. P. Chen, Y. Jung, C. T. Yavuz and A. Coskun, *Nat. Commun.*, 2013, **4**, 1357.
38 H. A. Patel, S. H. Je, J. Park, Y. Jung, A. Coskun and C. T. Yavuz, *Chem.–Eur. J.*, 2014, **20**, 772–780.
39 S. Gu, J. Guo, Q. Huang, J. He, Y. Fu, G. Kuang, C. Pan and G. Yu, *Macromolecules*, 2017, **50**, 8512–8520.
40 W. Wang, M. Zhou and D. Yuan, *J. Mater. Chem. A*, 2017, **5**, 1334–1347.
41 S. Nandi, U. Werner-Zwanziger and R. Vaidhyanathan, *J. Mater. Chem. A*, 2015, **3**, 21116–21122.
42 X. Zhu, S. M. Mahurin, S.-H. An, C.-L. Do-Thanh, C. Tian, Y. Li, L. W. Gill, E. W. Hagaman, Z. Bian, J.-H. Zhou, J. Hu, H. Liu and S. Dai, *Chem. Commun.*, 2014, **50**, 7933.
43 P. Arab, M. G. Rabbani, A. K. Sekizkardes, T. İslamoğlu and H. M. El-Kaderi, *Chem. Mater.*, 2014, **26**, 1385–1392.
44 P. Arab, E. Parrish, T. İslamoğlu and H. M. El-Kaderi, *J. Mater. Chem. A*, 2015, **3**, 20586–20594.
45 J. Lu and J. Zhang, *J. Mater. Chem. A*, 2014, **2**, 13831–13834.
46 J.-X. Zhou, X.-S. Luo, X. Liu, Y. Qiao, P. Wang, D. Mecerreyes, N. Bogliotti, S.-L. Chen and M.-H. Huang, *J. Mater. Chem. A*, 2018, **6**, 5608–5612.
47 B. Panić, T. Frey, M. Borovina, K. Konopka, M. Sambolec, I. Kodrin and I. Biljan, *Polymers*, 2023, **15**, 229.
48 A. M. Alloush, H. Abdulghani, H. A. Amasha, T. A. Saleh and O. C. S. Al Hamouz, *J. Ind. Eng. Chem.*, 2022, **113**, 215–225.
49 M. B. Gawande, S. N. Shelke, R. Zboril and R. S. Varma, *Acc. Chem. Res.*, 2014, **47**, 1338–1348.
50 E. Gabano and M. Ravera, *Molecules*, 2022, **27**, 4249.
51 B. Díaz de Greñu, J. Torres, J. García-González, S. Muñoz-Pina, R. de los Reyes, A. M. Costero, P. Amorós and J. V. Ros-Lis, *ChemSusChem*, 2021, **14**, 208–233.
52 Z. Alsudairy, N. Brown, C. Yang, S. Cai, F. Akram, A. Ambus, C. Ingram and X. Li, *Precis. Chem.*, 2023, **1**, 233–240.
53 T. Frey, B. Panić, P. Šutalo, M. Borovina, I. Biljan and I. Kodrin, *CrystEngComm*, 2023, **25**, 3870–3884.
54 Y. Xu, Z. Li, F. Zhang, X. Zhuang, Z. Zeng and J. Wei, *RSC Adv.*, 2016, **6**, 30048–30055.
55 R. Bera, M. Ansari, A. Alam and N. Das, *J. CO2 Util.*, 2018, **28**, 385–392.
56 X. Jiang, Y. Liu, J. Liu, Y. Luo and Y. Lyu, *RSC Adv.*, 2015, **5**, 98508–98513.
57 L. Tao, F. Niu, D. Zhang, J. Liu, T. Wang and Q. Wang, *RSC Adv.*, 2015, **5**, 96871–96878.
58 M. M. Abdelnaby, T. A. Saleh, M. Zeama, M. A. Abdalla, H. M. Ahmed and M. A. Habib, *ACS Omega*, 2022, **7**, 14535–14543.

59 R. Bera, M. Ansari, A. Alam and N. Das, *ACS Appl. Polym. Mater.*, 2019, **1**, 959–968.
60 F. M. Wisser, K. Eckhardt, D. Wisser, W. Böhlmann, J. Grothe, E. Brunner and S. Kaskel, *Macromolecules*, 2014, **47**, 4210–4216.
61 R. Dawson, E. Stöckel, J. R. Holst, D. J. Adams and A. I. Cooper, *Energy Environ. Sci.*, 2011, **4**, 4239.
62 N. Cindro, Ž. Car, V. Petrović Peroković, M. Borovina, B. Panić, I. Kodrin and I. Biljan, *Heliyon*, 2023, **9**, e21781.
63 A. Halder, S. Kandambeth, B. P. Biswal, G. Kaur, N. C. Roy, M. Addicoat, J. K. Salunke, S. Banerjee, K. Vanka, T. Heine, S. Verma and R. Banerjee, *Angew. Chem., Int. Ed.*, 2016, **55**, 7806–7810.
64 D. O. Ojwang, J. Grins and G. Svensson, *Microporous Mesoporous Mater.*, 2018, **272**, 70–78.
65 S. B. Singh and S. A. Dastgheib, *Carbon*, 2024, **228**, 119331.
66 S. B. Singh and M. De, *Mater. Chem. Phys.*, 2020, **239**, 122102.